

# 1 MSdb: an integrated expression atlas of human

## 2 musculoskeletal system

3 Junxin Lin<sup>1,2,3,4,8\*</sup>, Ruonan Tian<sup>2,8</sup>, Ziwei Xue<sup>2,8</sup>, Dengfeng Ruan<sup>1,2,5</sup>, Pengwei Chen<sup>2</sup>, Yiwen

4 Xu<sup>1,2,5</sup>, Chao Dai<sup>2</sup>, Weiliang Shen<sup>1,3,4,5,6</sup>, Hongwei Ouyang<sup>1,2,3,4,5,6\*</sup>, Wanlu Liu<sup>1,2,3,4,7\*</sup>,

5 1. Department of Orthopedic of the Second Affiliated Hospital of Zhejiang University  
6 School of Medicine, Zhejiang University, Hangzhou, Zhejiang, China,

7 2. Zhejiang University-University of Edinburgh Institute, Zhejiang University School of  
8 Medicine, Hangzhou, China.

9 3. Dr. Li Dak Sum & Yip Yio Chin Center for Stem Cells and Regenerative Medicine,  
10 Zhejiang University School of Medicine, Hangzhou, China

11 4. Key Laboratory of Tissue Engineering and Regenerative Medicine of Zhejiang Province,  
12 Hangzhou, Zhejiang, China

13 5. Department of Sports Medicine, Zhejiang University School of Medicine, Hangzhou,  
14 China

15 6. China Orthopedic Regenerative Medicine Group (CORMed), Hangzhou, China

16 7. Alibaba-Zhejiang University Joint Research Center of Future Digital Healthcare,  
17 Zhejiang University, Hangzhou

18 8. These authors contributed equally to this work.

19

20 \*Correspondence: [linjunxin@zju.edu.cn](mailto:linjunxin@zju.edu.cn) (J.L.), [hwoy@zju.edu.cn](mailto:hwoy@zju.edu.cn) (H.O.), and

21 [wanluliu@intl.zju.edu.cn](mailto:wanluliu@intl.zju.edu.cn) (W.L.)

22

## 23 Abstract

24 We introduce MSdb (<https://www.msdb.org.cn>), a database for visualization and integrated  
25 analysis of next-generation sequencing data from human musculoskeletal system, along with  
26 manually curated patient phenotype data. Systematic categorizing, standardized processing  
27 and freely accessible knowledge enables the reuse of public data. MSdb provides various  
28 types of analysis, including sample-level browsing of metadata information, gene/miRNA  
29 expression, and single-cell RNA-seq dataset. In addition, MSdb also allows integrated  
30 analysis for cross-samples and cross-omics analysis, including customized differentially-  
31 expressed gene/microRNA analysis, microRNA-gene network, scRNA-seq cross-  
32 sample/disease integration, and gene regulatory network analysis.  
33

## 34 Main

35 The prevalence and burden of musculoskeletal (MSK) disorders are extremely high all over  
36 the world<sup>1,2</sup>. With the advancement of next-generation sequencing (NGS), a huge amount of  
37 sequencing data has been generated, which accelerated the research of pathological  
38 mechanisms and the development of novel therapeutic approaches for MSK disorders<sup>3-6</sup>.  
39 However, dispersed distribution of relevant data sets among different repositories makes it  
40 challenging to analyze and compare them in a uniform way. Therefore, we developed the  
41 human musculoskeletal system database (MSdb), an integrated expression atlas specifically  
42 for the human MSK system, containing 33 diseases, 126 projects, 3,398 transcriptomes and  
43 microRNAomes at bulk level, as well as 2,833,779 transcriptomes at single-cell level (Fig. 1a  
44 and [Supplementary Fig. 1](#)). MSdb incorporates cross-repository metadata into controlled  
45 vocabulary and uniform format, enabling efficient retrieval of sample information  
46 ([Supplementary Table](#)). MSdb provides multiple built-in data exploration and analysis  
47 functionalities, including gene/microRNA expression browsing, customized differentially-  
48 expressed genes/miRNAs analysis, integrated microRNA-gene interaction networks, as well  
49 as integrated single-cell expression atlas and cell type-specific gene regulatory networks  
50 analysis ([Supplementary Fig. 2](#) and [Supplementary Video](#)). Furthermore, MSdb allows  
51 downloading of processed data sets and publication-quality plots, offering wet lab scientists  
52 powerful tools to browse and re-analyze the public datasets without technical barriers.  
53

54 MSdb enables users to retrieve sample information via consistent and validated metadata  
55 curated by orthopedists and bioinformatics scientists ([Supplementary Table](#)). Users can  
56 search the database using multiple parameters like project identifier, diseases, and tissue  
57 types in order to find data sets that match their interests ([Supplementary Fig. 3a](#)). In metadata,  
58 four types of information are available: (i) data set and publication identifiers, (ii) patient  
59 phenotypes, (iii) sample information and (iv) data pre-processing summary. These items  
60 enable users to evaluate the biological meaning, clinical relevance and data quality of the  
61 samples. Summary statistics of the metadata are also presented to show global patterns of  
62 the studies ([Supplementary Fig. 4](#)).  
63

64 At bulk level, MSdb integrates information at two aspects: (i) cross-tissue integration, (ii)  
65 cross-omics integration. For cross-tissue integration, samples were initially integrated by  
66 projects to generate gene or microRNA expression atlas, and then labelled by their tissue

65 types, diseases, cell types, and tissue positions. Users may explore the expression of genes  
66 or microRNAs by these labels ([Supplementary Fig. 5](#) and [Supplementary Fig. 6](#)). In [Fig. 1b](#),  
67 [c](#), uniform manifold approximation and projection (UMAP) plots show the integrated  
68 expression atlas of bulk RNA-seq or microRNA-seq data in MSdb, and samples are colored  
69 by representative tissue types and diseases. Feature plots and violin plots show that *COL3A1*,  
70 a connective tissue marker, was pervasively expressed in MSK tissues as expected ([Fig. 1b](#)  
71 and [Supplementary Fig. 5](#)). Cerebrospinal fluid from amyotrophic lateral sclerosis (ALS)  
72 patients showed enrichment of the potential diagnostic marker miR-4649-5p ([Fig. 1c](#) and  
73 [Supplementary Fig. 6](#))<sup>7</sup>. For cross-omics integration, MSdb enables users to analyze bulk  
74 RNA-seq and microRNA-seq data side-by-side and integrate the results to predict disease-  
75 related gene expression regulatory mechanisms. MSdb's differential expression analysis  
76 module allows users to choose two groups of samples for comparison ([Supplementary Fig.](#)  
77 [3b](#)). An interactive volcano plot can be used to explore differentially expressed genes or  
78 microRNAs between user-defined groups, and the expression level of a specific gene or  
79 microRNA can be queried and will be displayed in the box plot ([Supplementary Fig. 3b](#)). By  
80 integrating differentially expressed genes and microRNAs between normal and pathological  
81 intervertebral disks, we constructed a microRNA-gene interaction network ([Fig. 1d, e](#)). The  
82 network revealed previous reported (indicated by asterisk) and unanticipated disease-  
83 associated microRNAs and their potential gene targets, which can be interactively explored  
84 on our website ([Fig. 1e](#)). We demonstrated that the expression level of *miR-146a-5p* was  
85 down-regulated, while its target *SPP1* was up-regulated in degenerative intervertebral disks  
86 when compared to healthy control ([Fig. 1d, e](#)). Since abnormal expression of *SPP1* plays a  
87 critical role in the pathological process of intervertebral disk degeneration (IDD)<sup>8</sup>, our analysis  
88 indicated that targeting *SPP1* with *miR-146a-5p* mimic might be a therapeutic method to  
89 counteract disk degeneration. Collectively, MSdb offers users with integrated expression  
90 atlas and useful data analysis functionalities to understand gene function and regulation in  
91 homeostasis and diseases.

92 In recent years, the emergence of single-cell technology permits researchers to discover  
93 new and possibly unexpected biological findings relative to bulk-level profiling. Intriguingly,  
94 MSdb contains a wealth of single-cell RNA sequencing (scRNA-seq) data and provides a suit  
95 of functionalities for users to explore gene expression at single-cell level. For each scRNA-  
96 seq dataset, we provide textual and graphical representations for sample information, quality  
97 control metrics, unsupervised cell clustering, reference-based cell subtype prediction, as well  
98 as marker genes for each cell type ([Supplementary Fig. 7](#)). In a single-cell profiling of synovial  
99 tissue from a female patient with rheumatoid arthritis, major cell types, such as fibroblasts,  
100 macrophages, T cells and monocytes were identified and the specific *CD68* expression in the  
101 predicted macrophages (cluster 2) indicated the reliability of cell clustering and automated  
102 cell type prediction ([Supplementary Fig. 7a-h](#)). For more sophisticated cell type clustering  
103 and annotation, users can adjust leiden resolution for cell clustering and change reference  
104 dataset for cell type prediction ([Supplementary Fig. 7i](#)). To help with manual annotation, a  
105 heatmap and a table of marker genes are displayed and available for download.  
106 ([Supplementary Fig. 7j, k](#)).

107 We also implemented an in-house variational autoencoder (VAE) based deep-learning  
108 framework to facilitate the integrative analysis for scRNA-seq data sets from different studies.

109 **Fig. 2** displays the result of integrated analysis of single-cell gene expression data from  
110 healthy, osteoarthritis (OA), rheumatic arthritis (RA) and undifferentiated arthritis (UA)  
111 patients. Using the VAE model, we were able to remove batch differences and integrate  
112 heterogeneous data from different studies (**Fig. 2b**). The cell types could be identified by the  
113 known marker genes, whose expression patterns support that our integration method  
114 appropriately aligned gene expression for each cell types (**Fig. 2a, c**). Interestingly, we  
115 observed a distinct distribution pattern of fibroblasts from OA and RA patients (**Fig. 2b**).  
116 Differential expression analysis revealed that *IGFBP3* and *LOX* were more enriched in OA-  
117 derived fibroblast when compared to RA-derived fibroblast (**Fig. 2d**). *IGFBP3* and *LOX* were  
118 involved in extracellular matrix remodeling, which may determine synovial fibrosis and may  
119 be associated with the clinical symptoms of pain, hyperalgesia, and stiffness in osteoarthritis<sup>9</sup>.  
120 It was also noted that *CD74* and *HLA-DRA* were specifically expressed in RA fibroblasts,  
121 demonstrating an inflammatory state of fibroblasts that have been reported to be a major  
122 source of pro-inflammatory cytokines and highlighted as a potential therapeutic target in RA  
123 (**Fig. 2d**)<sup>10,11</sup>. Moreover, we inferred gene regulatory networks (GRNs) using a previously  
124 published deep regenerative model for each cell types<sup>12</sup>. Users may interactively visualize  
125 the GRNs in our database to explore the complicated molecular interactions governing  
126 potential cell identity (**Supplementary Fig. 8**).

127 Overall, MSdb is a resource created for the MSK research community and aims to fulfill  
128 the findability, accessibility, interoperability, and reusability (FAIR) principles of scholarly  
129 data<sup>13</sup>. The uniformity of sample information in MSdb enables metadata-based and database-  
130 scale analysis. MSdb's utility will continue to grow as public NGS data sets of human  
131 musculoskeletal system expand. We envision that it will broaden the use of human MSK data  
132 sets and will be invaluable to researchers in the MSK field.

133  
134

## 135 **Methods**

### 136 **Data collection and meta information curation**

137 Bulk RNA-seq, microRNAs-seq and single-cell RNA-seq data of human musculoskeletal  
138 system were originated from NCBI Gene Expression Omnibus (GEO) and EMBL's European  
139 Bioinformatics Institute (EMBL-EBI)<sup>14,15</sup>. We manually curated both GEO and EMBL-EBI-  
140 derived sample information to provide a coherent and standardized metadata. The resulting  
141 collection offers the following information for each dataset. 'SampleName' contains the  
142 sample's identification code in GEO (e.g. GSM2112324) or EMBL-EBI (e.g. ERS1034560).  
143 'ProjectID' contains the sample's project identification code in GEO (e.g. GSE80072) or  
144 EMBL-EBI (e.g. E-MTAB-4304). 'Publication\_DOI' contains the digital object identifier of the  
145 original publication. 'Category' indicates the MSK tissues that the datasets are related to.  
146 'AssayType' indicates which sequencing types were implemented on the samples.  
147 'LibraryLayout' refers to pair-end sequencing or single-end sequencing. 'Disease' contains  
148 the information about the diseases or health status. 'SourceTissue\_type' indicates tissue  
149 sources of the biological materials used for sequencing. 'Sourcetissue\_condition' indicates  
150 whether the tissues are pathological or normal. 'SourceTissue\_position' refers to a more  
151 specific anatomical location of the 'SourceTissue\_type'. 'SourceTissue\_celltype' indicates

152 whether whole tissue or a specific cell type in the tissue was used for sequencing. 'OtherInfo'  
153 contains other information that can help users to evaluate the biological or clinical relevance  
154 of the data, such as whether the patients were response to treatment. 'Age', 'AgeGroup' and  
155 'Gender' of the patients are also presented, if available. To assist evaluating the quality of  
156 the datasets, we also provide the following information related to data quality assessment  
157 along with metadata: sequencing library preparation kit ('LibraryPrepKit'), average spot length  
158 ('AvgSpotLen'), sequencing instrument ('Instrument'), total reads ('TotalReads'), uniquely  
159 mapped reads ('UniquelyMappedReads'), percentage of uniquely mapped reads  
160 ('UniquelyMappedReads%'), percentage of multiple mapped loci ('MultipleLoci%').

161

## 162 **Bulk RNA-seq and microRNA-seq processing and data analysis**

163 Quality control (QC) of raw sequencing reads for each project was performed by FastQC  
164 (v0.11.9)<sup>16</sup>. Cutadapt (v3.7) was used to find and remove adapter sequences, primers, low  
165 quality sequence and other types of unmated sequences<sup>17</sup>. For bulk RNA-seq, the trimmed  
166 reads were mapped to the reference index built on human genome assembly GRCh38 (hg38,  
167 [http://ensembl.org/Homo\\_sapiens/](http://ensembl.org/Homo_sapiens/)) using STAR (v2.7.9a) and counts were summarized to  
168 the genomic protein coding genes by featureCounts (v2.0.3)<sup>18,19</sup>. For microRNA-seq, trimmed  
169 reads were mapped to the reference index built on miRbase hairpins and Samtools (v1.14)  
170 was used to report alignment summary statistics and calculate the microRNA counts<sup>20</sup>. Batch  
171 effect between different studies was estimated and adjusted by ComBat-seq<sup>21</sup>. Then, all bulk  
172 RNA-seq gene counts and microRNA-seq counts were merged, respectively. To show  
173 sample correlation, Scanpy (1.9.1) was used to reduce dimension and generate uniform  
174 manifold approximation and projection (UMAP)<sup>22</sup>. To perform differential expression analysis,  
175 a t-test was applied to the normalized RPKM or RPM data and a false discovery rate (FDR)  
176 adjusted p-value was canulated using Benjamini–Hochberg method.

177 The MSdb's online differential expression analysis tool (<https://www.msdb.org.cn/browse/>)  
178 was used to obtain differentially expressed mRNAs and miRNAs (FDR < 0.01 and fold  
179 change > 2). Down-regulated microRNAs and up-regulated genes in degenerative  
180 intervertebral disks were used for further analysis. CyTargetLinker (v4.1.0) was used to  
181 predict and construct the miRNA-gene interaction network with miRTarBase Homo sapiens  
182 release 8.0 linksets was used as a reference<sup>23,24</sup>. Cytoscape software (v3.9.1) was used for  
183 miRNA-mRNA regulatory network visualization<sup>25</sup>.

184

## 185 **Single cell RNA-seq processing and data analysis**

186 The genome reference used in scRNA-seq analysis is GRCh38. For droplet-based scRNA-  
187 seq, the raw data were processed using Cell Ranger (v7.0.0) or Drop-seq\_tools with standard  
188 pipeline and default parameters to obtain gene expression matrix<sup>26,27</sup>. For full-length scRNA-  
189 seq, the data were mapped using STAR (v2.7.9a) and quantified using featureCounts (v2.0.3).  
190 To perform downstream analysis, the gene expression matrix containing UMI counts was  
191 read into an AnnData object by Scanpy (v1.9.1) in Python3 (v3.9.12)<sup>22</sup>. Cells with unique  
192 gene counts less than 200 or genes that are detected in less than 3 cells were removed. To  
193 perform unsupervised cell clustering analysis, the UMI counts were normalized to counts per  
194 million (CPM) with `scanpy.pp.normalize_total` function, followed by log-transformation and  
195 principal component analysis (PCA) using `scanpy.pp.log1p` and `scanpy.tl.pca` functions. The

196 neighborhood graph was calculated based on the PCA results using  
197 *scipy.pp.neighbors* function and the Leiden algorithm was used to perform unsupervised  
198 cell clustering (*scipy.tl.leiden*)<sup>28</sup>. Marker genes for each cell cluster were identified by  
199 *sc.tl.rank\_genes\_groups* function. To perform reference-based cell subtype prediction, the  
200 filtered count matrix was loaded into Seurat (v4.1.1) in R (v4.2.0)<sup>29</sup>. The annotation of cell  
201 subtype was performed by SingleR (v1.10.0) R-package using different references, including  
202 the BlueprintEncodeData and the HumanPrimaryCellAtlasData<sup>30</sup>. Marker genes for each  
203 annotated cell types were identified by *FindAllMarkers* in Seurat package. UMAP was used  
204 for the data visualization of unsupervised cell clustering, cell type prediction and marker gene  
205 expression.

206 We built a single-cell atlas of the synovium containing 101,610 cells from 3 studies and  
207 34 samples. We have implemented a probabilistic model based on a variational autoencoder  
208 to integrate single-cell RNA-seq datasets and remove batch effects, accepting raw count  
209 matrix as input. The variational distribution adopts the log-normal distribution with scalar  
210 mean and variance output from the encoder, regularized by the Kullback–Leibler divergence.  
211 The decoder takes categorical encoding of the sample name to reflect biological variance  
212 and remove batch effects. The count data is modelled by the zero-inflated binomial  
213 distribution. The dimension of the latent embedding of the variational autoencoder was  
214 chosen to be 10. The top 3,000 highly variable genes were selected using Scanpy (v1.9.1)  
215 for the model to learn the latent embeddings<sup>22</sup>. The model was trained on NVIDIA GeForce  
216 RTX 3090 addressing 24 GB RAM. Cell annotations for the integrated datasets were based  
217 on unsupervised clustering result and prior knowledge of marker gene expression of major  
218 cell types including B cells, T/NK cells, macrophages, monocytes, fibroblasts, endothelial  
219 cells and smooth muscle cells. The final representation of the dataset was projected to 2-  
220 dimensional space using the UMAP algorithm.  
221

## 222 **Website development**

223 We developed a user-friendly web interface with advanced functions to present our uniformly  
224 curated metadata and NGS data. The front-end interface was developed with HTML5 and  
225 CSS3 languages, based on the BootStrap (v5.2.1) toolkit. All font-end tables were built  
226 through DataTables (v1.12.1), a plug-in for the jQuery Javascript library. All data  
227 visualizations were developed by D3.js (v7), a JavaScript library for document manipulation.  
228 All back-end data including the bulk RNA-seq and microRNA-seq gene count matrix, UMAP  
229 coordinate information, the scRNA-seq clusters, cell subtype annotation, marker genes for  
230 different clusters were maintained into PostgreSQL database management system (v14.5).  
231 The MSdb database is deployed with a Nginx web server (v1.18.0) on an Ubuntu Linux  
232 (v20.04.5 LTS) operating system.  
233

## 234 **Acknowledgements**

235 The authors would like to thank all researchers who generated the data sets that are collected,  
236 analyzed, and displayed in MSdb. We thank Dr. Xiao Chen, Dr. Zi Yin, Dr. Wenyan Zhou, Dr.  
237 Dr. Can Zhang, Dr. Xiaolei Zhang, Fan Jiayi, and clinicians Yan Wu (M.D.), Dr. Yejun Hu  
238 (M.D.), Dr. Kun Zhao (M.D.), Dr. Yuzi Xu (M.D.) and Dr. Geyu Gu (M.D.) for their helpful

239 discussions and valuable suggestions. We would also like to thank the technical support  
240 provided by the Core Facilities, especially the ZJE server of ZJU-UoE Institute. This work  
241 was funded by National Natural Science Foundation of China [32170551 to L.W.; T2121004  
242 to H.O.]; Fundamental Research Funds for the Central Universities 226-2022-00134 (to W.L.);  
243 Alibaba Cloud [to L.W.].  
244

## 245 **Author contributions**

246 J.L., W.L., H.O., and W.S. conceived the study and designed database. R.T., P.C., C.D., and  
247 J.L. collected and processed the data. R.T., D.R., Y.X. and J.L. curated the metadata. R.T.  
248 and Z.X. developed the database and web server. R.T., Z.X., D.R., J.L., and W.L. analyzed  
249 the data. R.T., Z.X., D.R., W.L. and J.L. wrote the manuscript. All authors contributed to the  
250 review and corrections of the manuscripts.  
251

## 252 **Data availability**

253 All raw data are available on GEO (<https://www.ncbi.nlm.nih.gov/geo/>) and EMBL-EBI  
254 (<https://www.ebi.ac.uk/>) repositories. All curated sample information and processed bulk  
255 RNA-seq and microRNA-seq data can be downloaded from the MSdb database  
256 (<https://www.msdb.org.cn>). Single-cell RNA-seq matrices are available upon reasonable  
257 request.  
258

## 259 **Code availability**

260 We used publicly available software to process and analyze data, which are listed and  
261 described in Methods. Code for VAE used in this paper for data integration can be found at  
262 [https://github.com/wanluliu/2022\\_MSdb\\_code](https://github.com/wanluliu/2022_MSdb_code).  
263

264 **Competing interests.** The authors declare no competing interest.  
265

## 266 **References**

- 267 1. Cieza, A., *et al.* Global estimates of the need for rehabilitation based on the Global Burden of Disease  
268 study 2019: a systematic analysis for the Global Burden of Disease Study 2019. *Lancet* **396**, 2006-2017  
269 (2021).
- 270 2. Jin, Z., *et al.* Incidence trend of five common musculoskeletal disorders from 1990 to 2017 at the global,  
271 regional and national level: results from the global burden of disease study 2017. *Ann Rheum Dis* **79**,  
272 1014-1022 (2020).
- 273 3. Soul, J., *et al.* Stratification of knee osteoarthritis: two major patient subgroups identified by genome-  
274 wide expression analysis of articular cartilage. *Ann Rheum Dis* **77**, 423 (2018).
- 275 4. Yuan, C., *et al.* Classification of four distinct osteoarthritis subtypes with a knee joint tissue  
276 transcriptome atlas. *Bone Res* **8**, 38 (2020).
- 277 5. Xi, H., *et al.* A Human Skeletal Muscle Atlas Identifies the Trajectories of Stem and Progenitor Cells  
278 across Development and from Human Pluripotent Stem Cells. *Cell Stem Cell* **27**, 181-185 (2020).

279 6. Nicolle, R., *et al.* Integrated molecular characterization of chondrosarcoma reveals critical determinants  
280 of disease progression. *Nat Commun* **10**, 4622 (2019).

281 7. Takahashi, I., *et al.* Identification of plasma microRNAs as a biomarker of sporadic Amyotrophic Lateral  
282 Sclerosis. *Mol Brain* **8**, 67 (2015).

283 8. Marfia, G., *et al.* Gene expression profile analysis of human mesenchymal stem cells from herniated  
284 and degenerated intervertebral discs reveals different expression of osteopontin. *Stem Cells Dev* **24**,  
285 320-328 (2015).

286 9. Zhang, L., *et al.* Synovial Fibrosis Involvement in Osteoarthritis. *Front Med (Lausanne)* **8**, 684389 (2021).

287 10. Filer, A. The fibroblast as a therapeutic target in rheumatoid arthritis. *Curr Opin Pharmacol* **13**, 413-419  
288 (2013).

289 11. Zhang, F., *et al.* Defining inflammatory cell states in rheumatoid arthritis joint synovial tissues by  
290 integrating single-cell transcriptomics and mass cytometry. *Nat Immunol* **20**, 928-942 (2019).

291 12. Shu, H., *et al.* Modeling gene regulatory networks using neural network architectures. *Nature  
292 Computational Science* **1**, 491-501 (2021).

293 13. Wilkinson, M.D., *et al.* The FAIR Guiding Principles for scientific data management and stewardship.  
294 *Sci Data* **3**, 160018 (2016).

295 14. Barrett, T., *et al.* NCBI GEO: archive for functional genomics data sets--update. *Nucleic Acids Res* **41**,  
296 D991-995 (2013).

297 15. Madeira, F., *et al.* Search and sequence analysis tools services from EMBL-EBI in 2022. *Nucleic Acids  
298 Res* (2022).

299 16. Andrews, S. FastQC: A Quality Control Tool for High Throughput Sequence Data [Online]. (2010).  
300 Available online at: <http://www.bioinformatics.babraham.ac.uk/projects/fastqc/>

301 17. Martin, M. Cutadapt removes adapter sequences from high-throughput sequencing reads. *2011* **17**, 3  
302 (2011).

303 18. Liao, Y., Smyth, G.K. & Shi, W. featureCounts: an efficient general purpose program for assigning  
304 sequence reads to genomic features. *Bioinformatics* **30**, 923-930 (2014).

305 19. Dobin, A., *et al.* STAR: ultrafast universal RNA-seq aligner. *Bioinformatics* **29**, 15-21 (2013).

306 20. Li, H., *et al.* The Sequence Alignment/Map format and SAMtools. *Bioinformatics* **25**, 2078-2079 (2009).

307 21. Zhang, Y., Parmigiani, G. & Johnson, W.E. ComBat-seq: batch effect adjustment for RNA-seq count  
308 data. *NAR Genom Bioinform* **2**, lqaa078 (2020).

309 22. Wolf, F.A., Angerer, P. & Theis, F.J. SCANPY: large-scale single-cell gene expression data analysis.  
310 *Genome Biol* **19**, 15 (2018).

311 23. Kutmon, M., Ehrhart, F., Willighagen, E.L., Evelo, C.T. & Coort, S.L. CyTargetLinker app update: A  
312 flexible solution for network extension in Cytoscape. *F1000Res* **7**(2018).

313 24. Hsu, S.D., *et al.* miRTarBase: a database curates experimentally validated microRNA-target interactions.  
314 *Nucleic Acids Res* **39**, D163-169 (2011).

315 25. Shannon, P., *et al.* Cytoscape: a software environment for integrated models of biomolecular interaction  
316 networks. *Genome Res* **13**, 2498-2504 (2003).

317 26. Zheng, G.X., *et al.* Massively parallel digital transcriptional profiling of single cells. *Nat Commun* **8**,  
318 14049 (2017).

319 27. Macosko, E.Z., *et al.* Highly Parallel Genome-wide Expression Profiling of Individual Cells Using  
320 Nanoliter Droplets. *Cell* **161**, 1202-1214 (2015).

321 28. Traag, V.A., Waltman, L. & van Eck, N.J. From Louvain to Leiden: guaranteeing well-connected  
322 communities. *Sci Rep* **9**, 5233 (2019).

323 29. Hao, Y., *et al.* Integrated analysis of multimodal single-cell data. *Cell* **184**, 3573-3587 e3529 (2021).

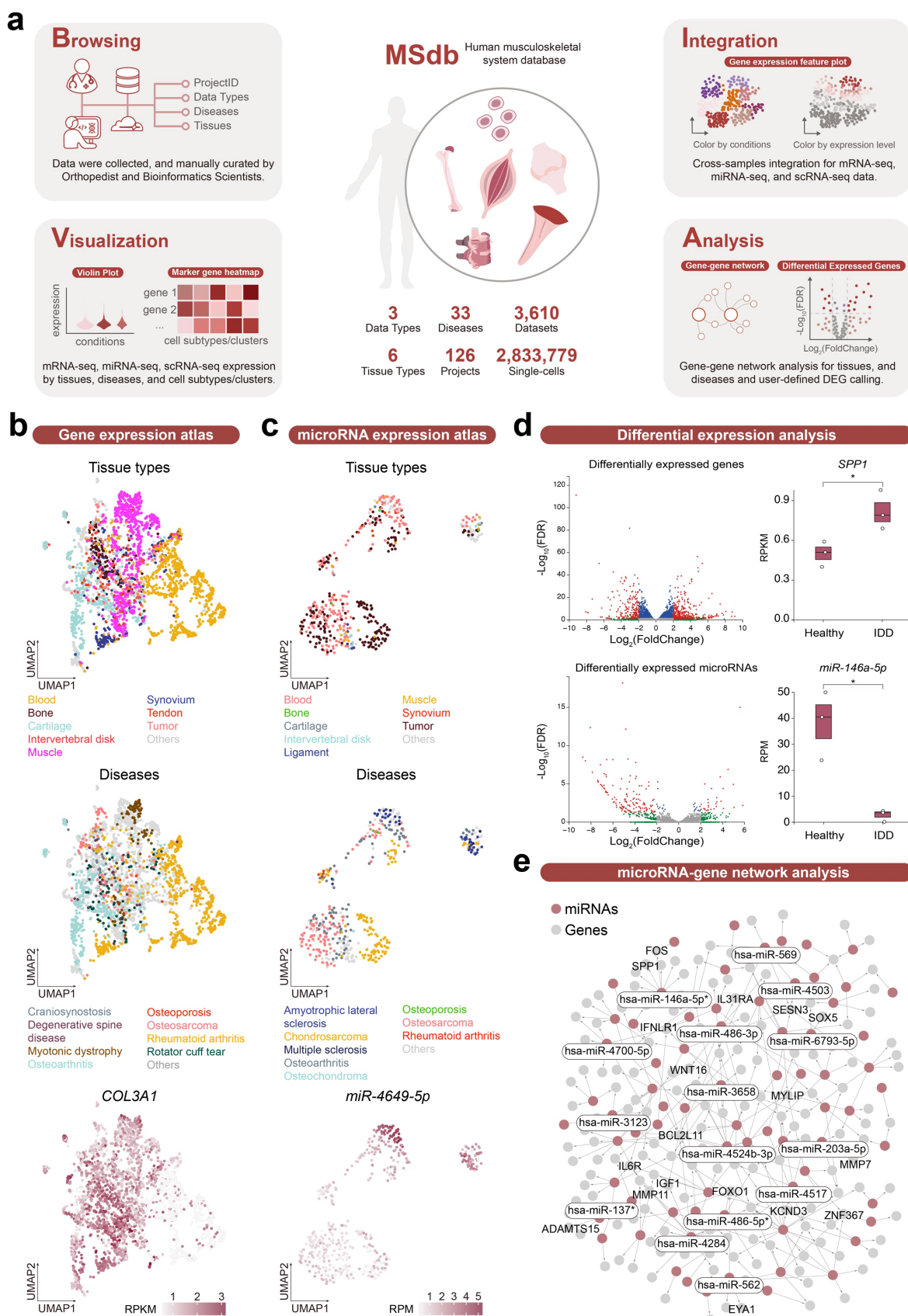
324 30. Aran, D., *et al.* Reference-based analysis of lung single-cell sequencing reveals a transitional profibrotic

325 macrophage. *Nat Immunol* **20**, 163-172 (2019).

326

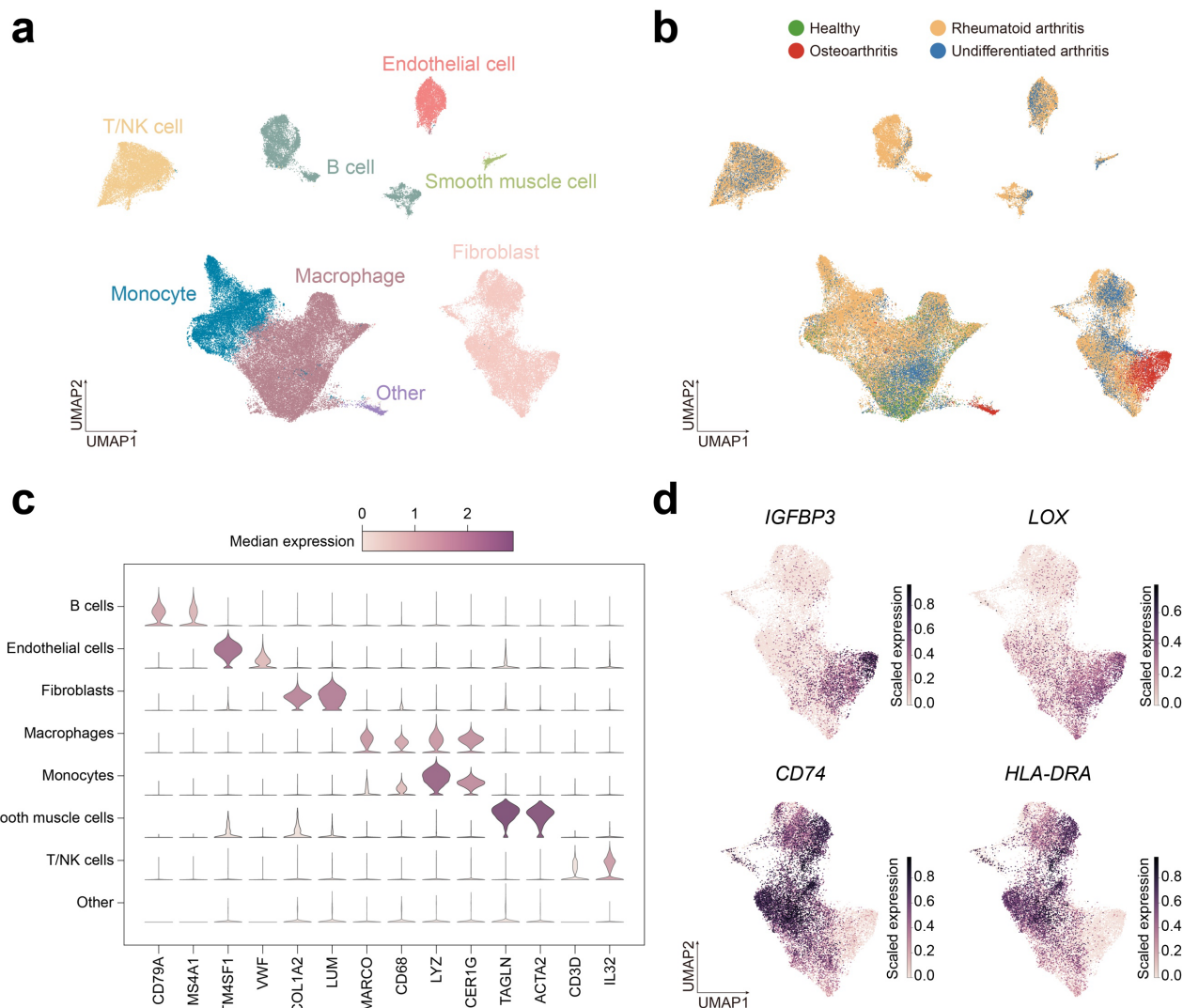
327

## Figures and legends



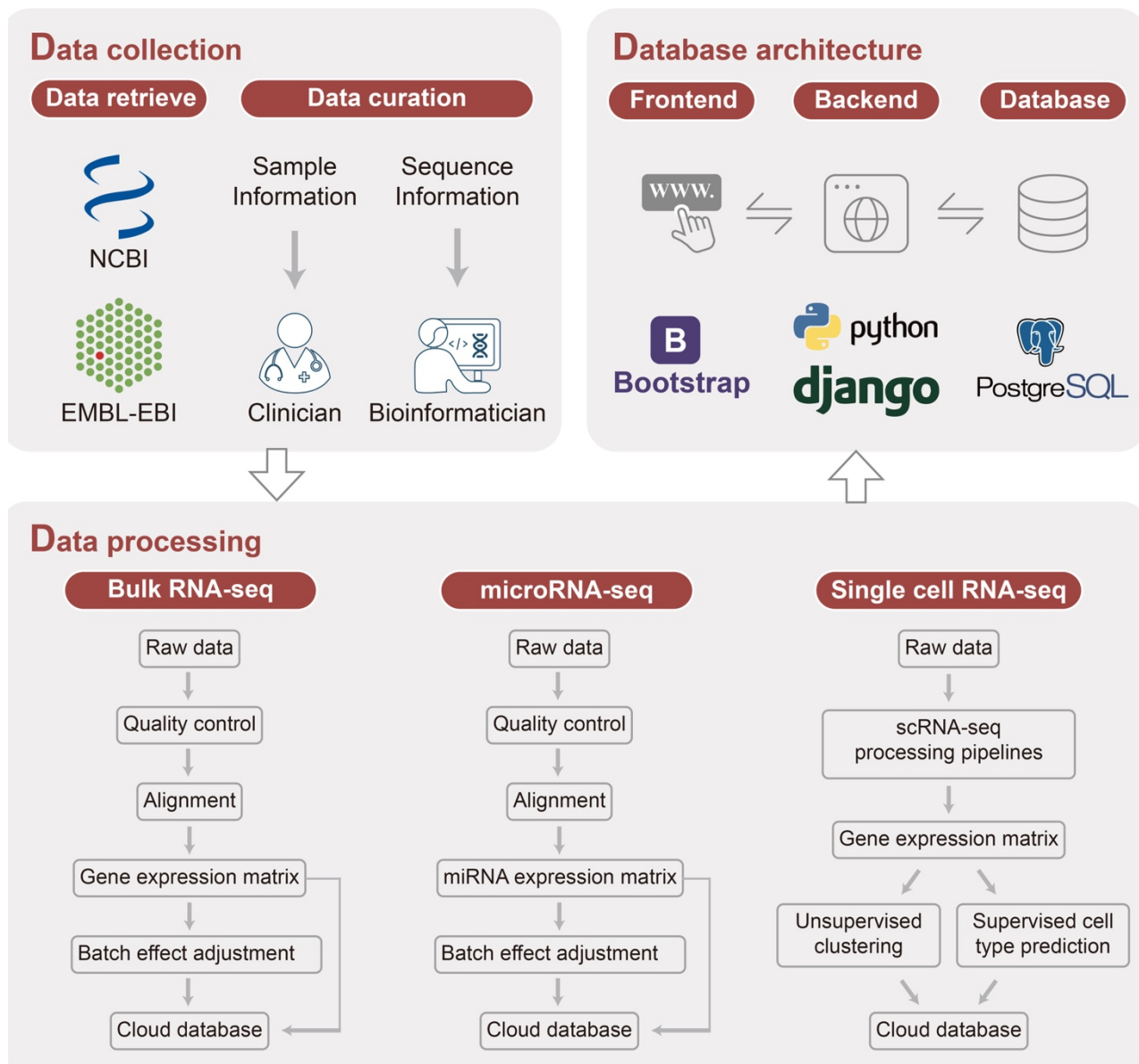
330 **Fig. 1. MSdb framework and illustrative data analysis. a,** Overview of MSdb. MSdb is a  
331 comprehensive database of next-generation sequencing data on human musculoskeletal system tissues  
332 and cells, enhanced with manually curated patient phenotypes, advanced analysis and visualization  
333 tools. **b, c,** UMAP plots showing gene (**b**) and microRNA (**c**) expression atlas in MSdb. All gene or  
334 microRNA expression data in MSdb were used for clustering, respectively. Samples are colored by tissue  
335 types (top), diseases (middle) and *COL3A1/miR-4649-5p* expression levels (bottom). **d,** Volcano plots  
336 and box plots showing dysregulated genes (top) or microRNAs (bottom) between healthy (n=3) and  
337 degenerative (n=3) intervertebral disks. RPKM: reads per kilobase per million mapped reads; RPM:  
338 reads per million mapped reads. \*: FDR < 0.01. **e,** microRNA-gene interaction network built with down-  
339 regulated microRNAs and up-regulated genes in degenerative intervertebral disks. Red dots represent  
340 the microRNAs and grey dots represent the genes. Complete and interactive plots of the network are  
341 available online on MSdb database.

342  
343  
344  
345



354

## Supplementary figures and legends



355

356

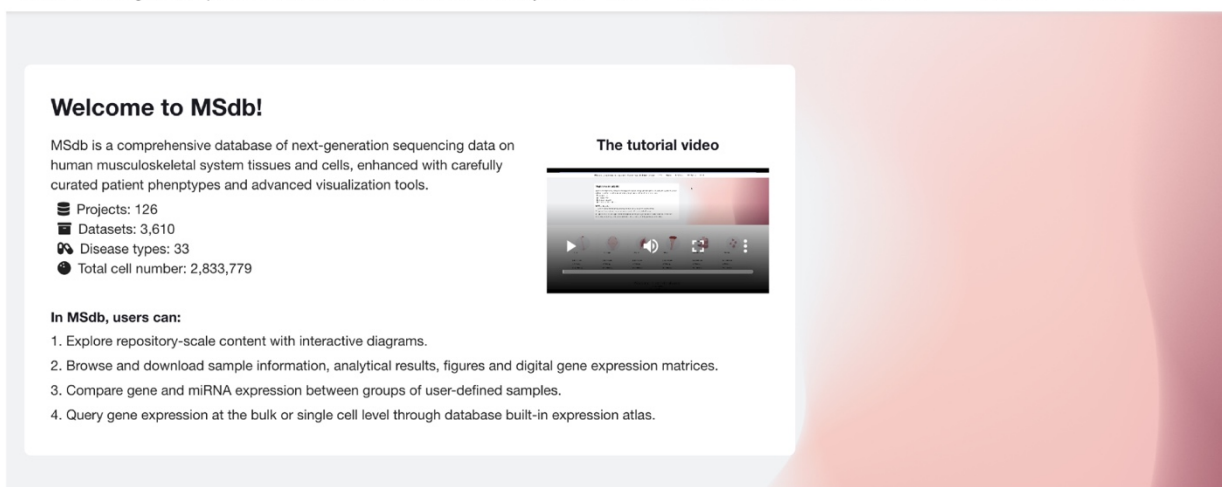
357 **Supplementary Fig. 1. Overview of MSdb database construction.** Publicly available data sets were  
358 collected from NCBI and EMBL-EBI databases. Metadata was curated by clinician and bioinformatician.  
359 Standardized data processing pipelines were built for bulk RNA-seq, microRNA-seq and single-cell RNA-  
360 seq. All processed data were stored in PostgreSQL database, and can be accessed with a user-friendly  
361 web interface.

362

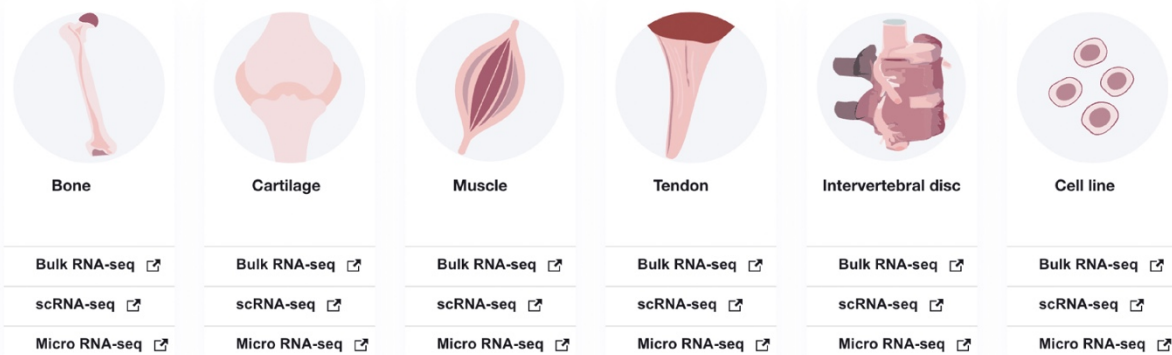
363

**a**

MSdb: an integrated expression atlas of human musculoskeletal system [Home](#) [Browse & Analysis](#) [Data Explorer](#) [Statistics](#) [About](#)



**b**



364

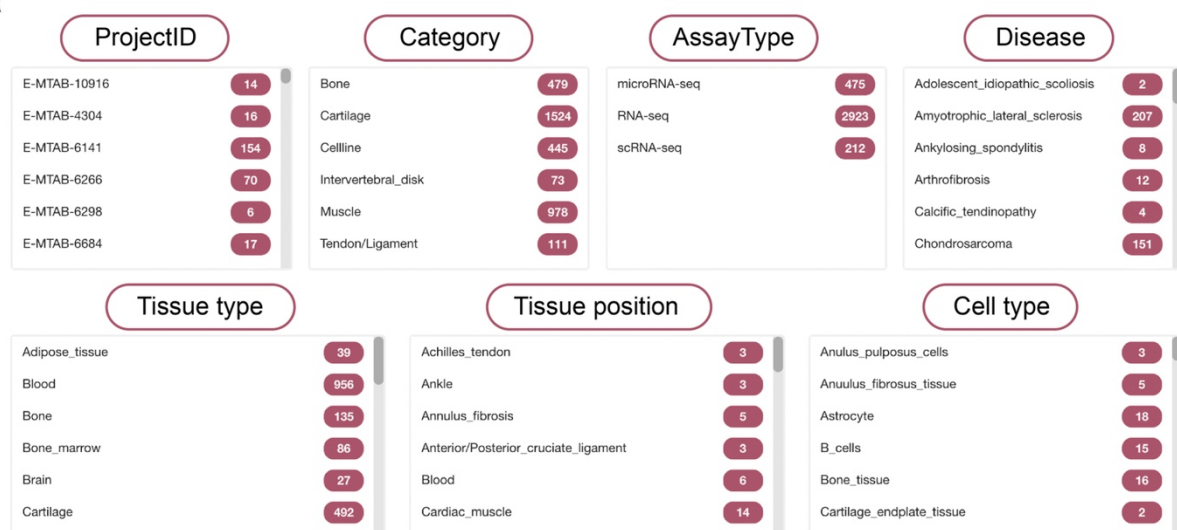
365

366 **Supplementary Fig. 2. An illustration of the MSdb home page. a, The upper portion of the home page**  
367 **showing site-wide menu choices and brief introduction of the database. b, The lower portion of the home**  
368 **page showing tissue icons and links for quick access to each data type.**

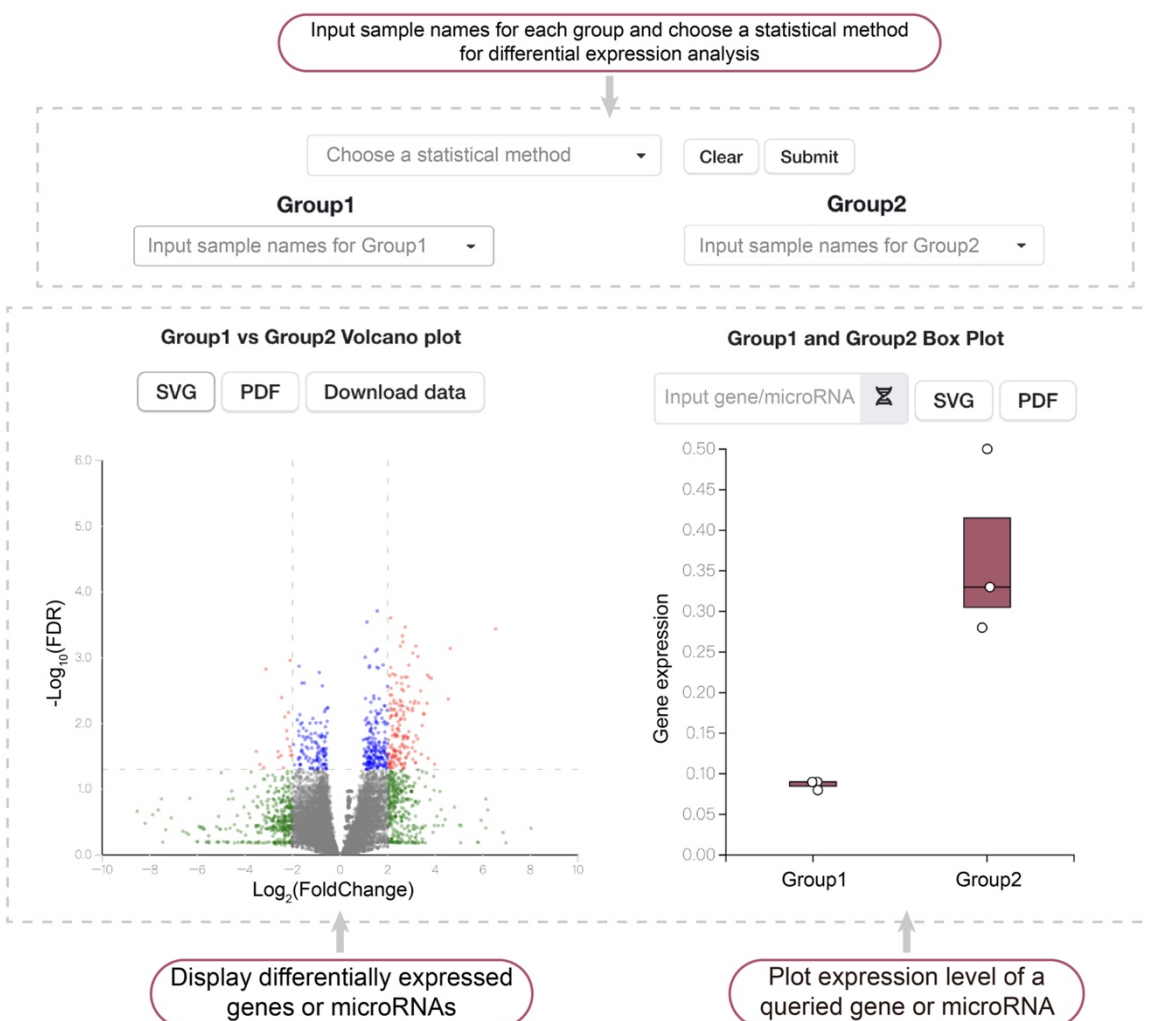
369

370

**a**



**b**



371

372

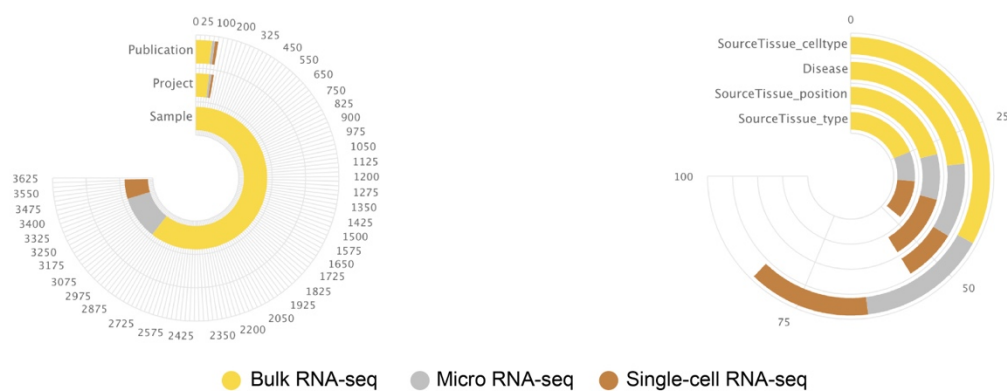
373

374

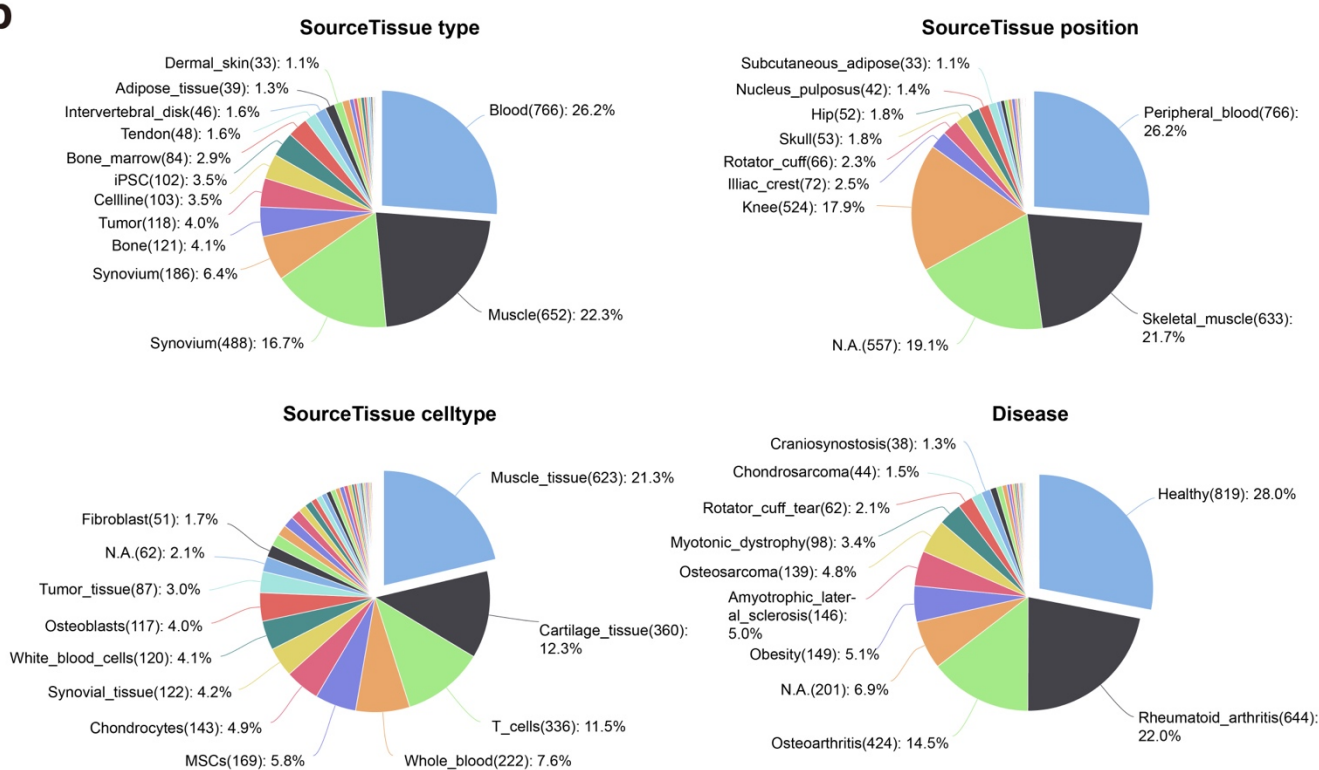
375

376 **Supplementary Fig. 3. An illustration of browse and differential expression analysis modules. a,**  
377 The selection boxes. Users can select data sets based on the project ID, tissue type, assay type, disease,  
378 source tissue type, source tissue position or source tissue cell type. **b,** The differential expression analysis  
379 module. Users may choose no more than 8 samples for each group. The differentially expressed genes  
380 between the user-defined samples will be calculated and presented in a volcano plot. Users may query  
381 the expression level of a specific gene or microRNA in the box plot.  
382

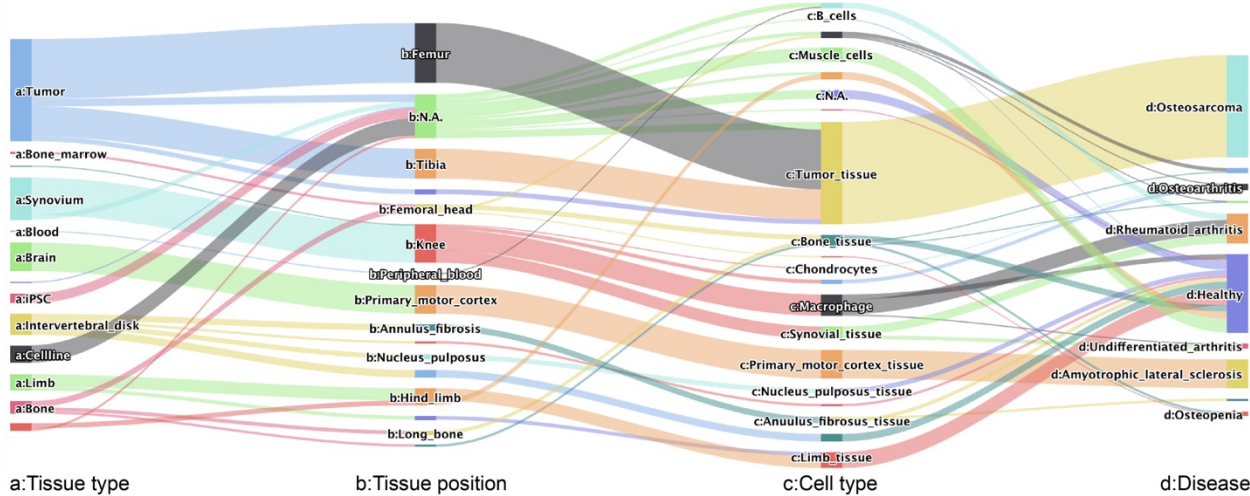
**a**



**b**



**c**

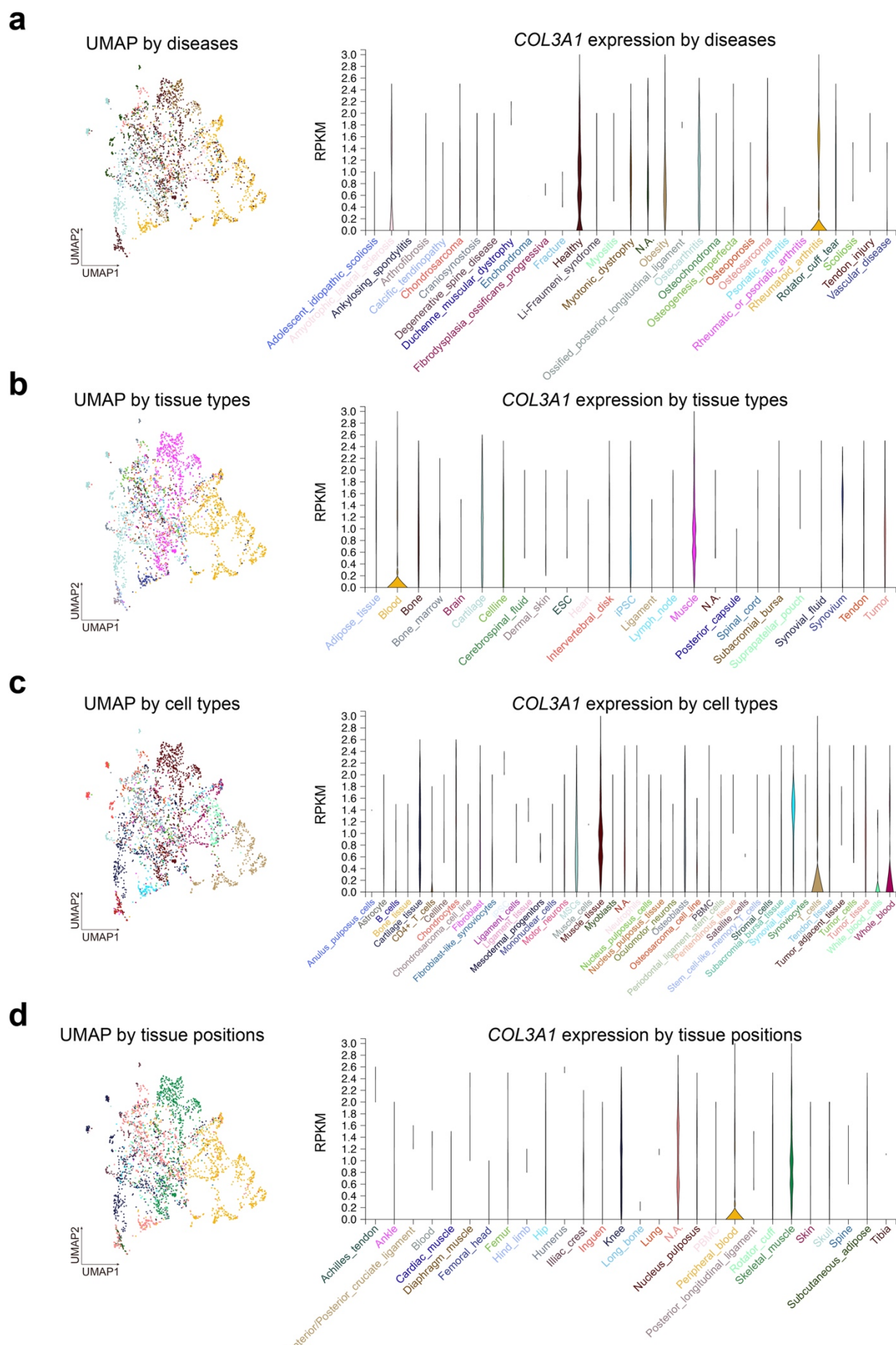


385 **Supplementary Fig. 4. An illustration of data statistics on MSdb.** **a**, The circular bar plots showing the  
386 number of publications, projects and samples (left), as well as the number of diseases, tissue types,  
387 positions and cell types (right) in MSdb. **b**, Pie charts showing the distribution of samples across tissue  
388 types, tissue positions, cell types and diseases. Shown are the statistics of bulk RNA-seq, and the statistics  
389 of other assay types can be found on our website. **c**, Sankey diagram displaying Tissue type - Tissue  
390 position - Cell type - Disease relationships of the samples. Shown is the diagram of scRNA-seq, and the  
391 diagrams of other assay types can be found on our website.

392

393

394



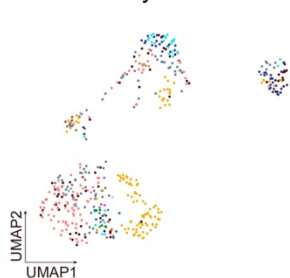
396 **Supplementary Fig. 5. Sample clustering and gene expression plots of bulk RNA-seq.** UMAP plots  
397 and violin plots showing sample clustering and *COL3A1* expression by diseases (**a**), tissue types (**b**), cell  
398 types (**c**) and tissue positions (**d**). The color code of UMAP in each panel are indicated by the colors of the  
399 text below the violin plots.

400

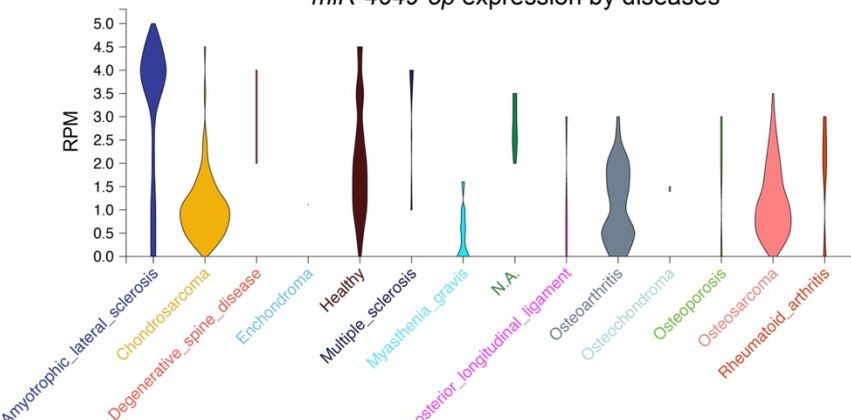
401

**a**

UMAP by diseases

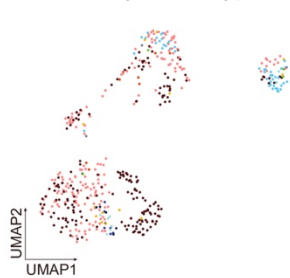


*miR-4649-5p* expression by diseases

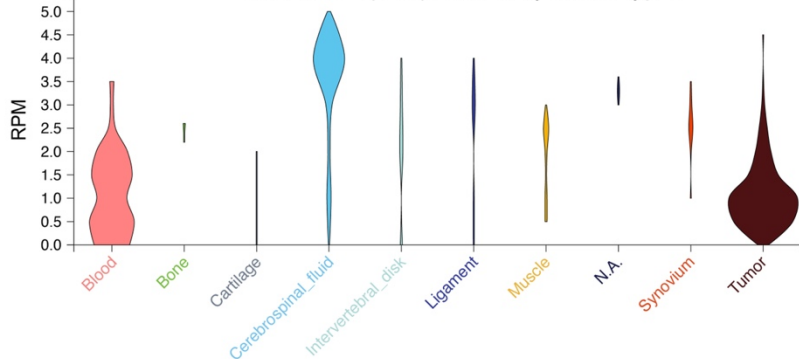


**b**

UMAP by tissue types

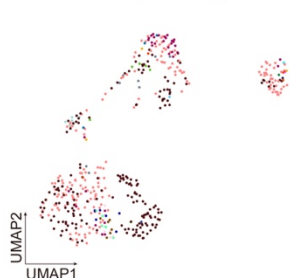


*miR-4649-5p* expression by tissue types

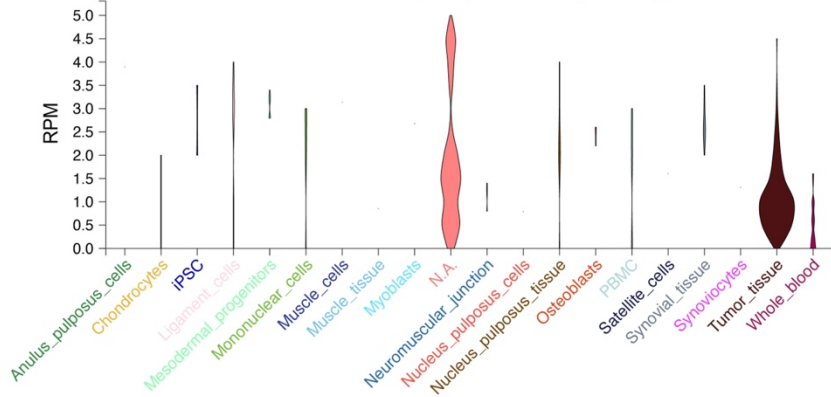


**c**

UMAP by cell types

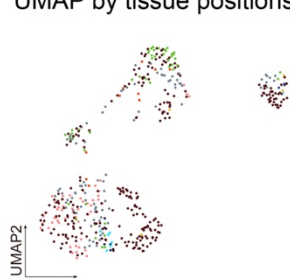


*miR-4649-5p* expression by cell types

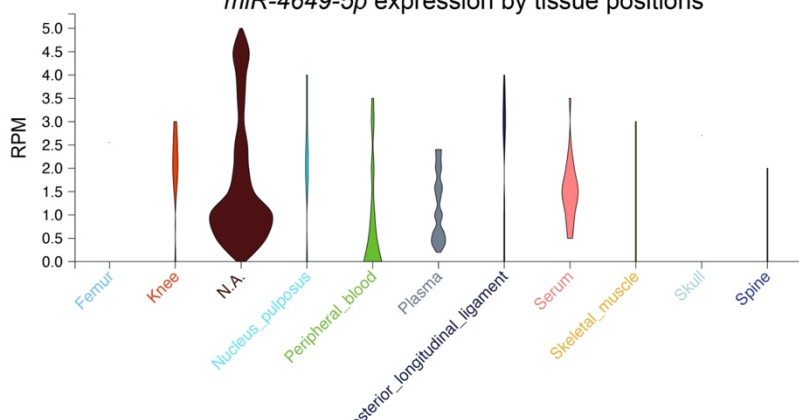


**d**

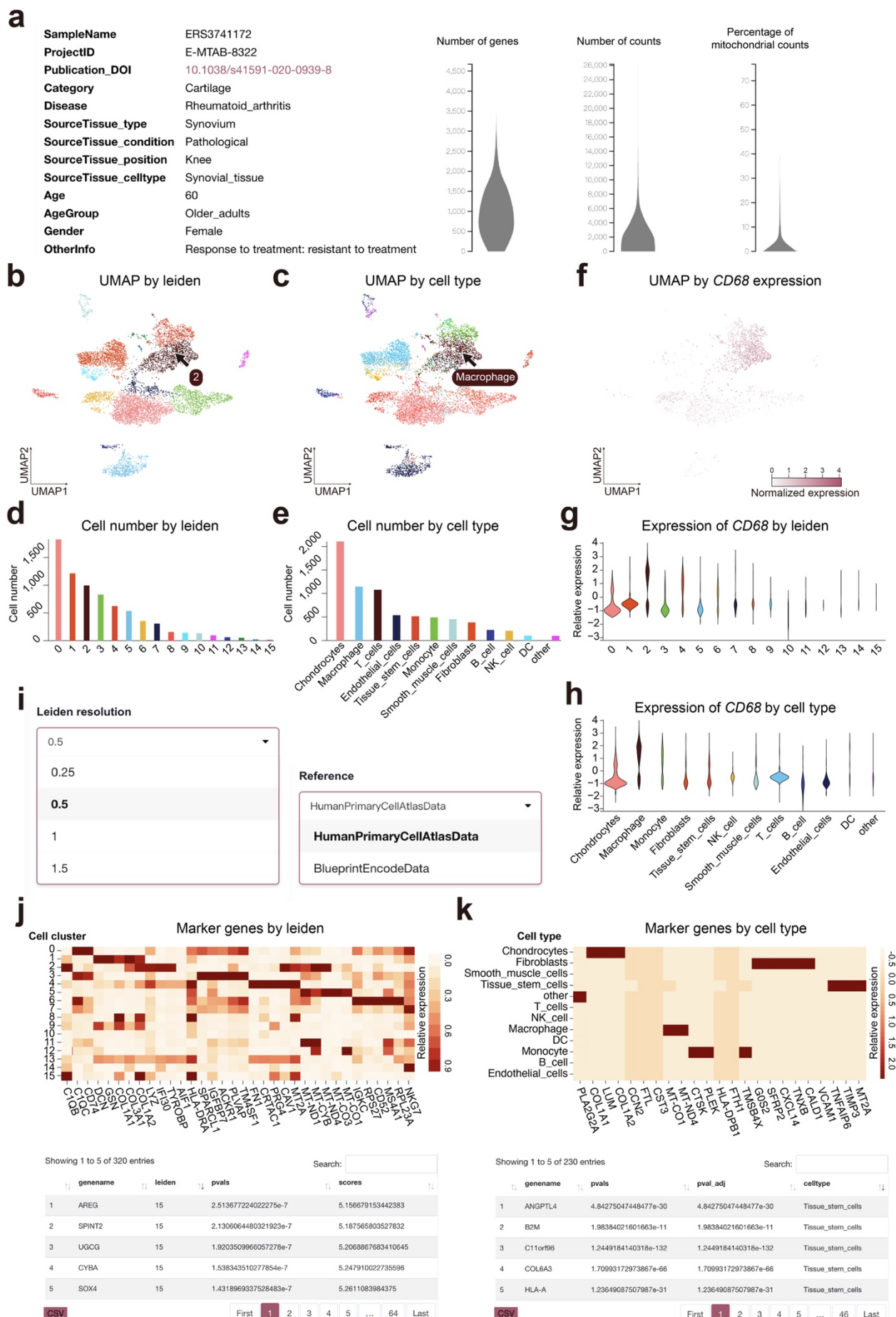
UMAP by tissue positions



*miR-4649-5p* expression by tissue positions



403 **Supplementary Fig. 6. Sample clustering and microRNA expression plots of microRNA-seq.** UMAP  
404 plots and violin plots showing sample clustering and *miR-4649-5p* expression by diseases **(a)**, tissue types  
405 **(b)**, cell types **(c)** and tissue positions **(d)**. The color code of UMAP in each panel are indicated by the  
406 colors of the text below the violin plots.  
407  
408  
409  
410  
411

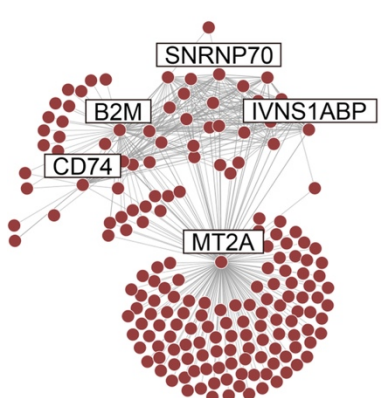


413 **Supplementary Fig. 7. An illustration of scRNA-seq expression atlas in MSdb.** **a**, Metadata and  
414 quality control metrics of the selected scRNA-seq dataset. **b, c**, UMAP plots showing unsupervised cell  
415 clustering (**b**) and cell type prediction (**c**) results. On web interface, the name of the cell cluster or cell type  
416 will be shown if one hovers the cursor on the dot. **d, e**, Cell number in each cell cluster (**d**) and predicted  
417 cell type (**e**). **f**, UMAP plot showing expression level of *CD68* gene in each single cell. **g, h**, Violin plots  
418 showing expression level of *CD68* gene in each cell cluster (**g**) and predicted cell type (**h**). **i**, Dropdown  
419 boxes offering choice for Leiden resolution (left) and reference data sets (right) for cell clustering and cell  
420 type prediction, respectively. **j, k**, The heatmap and table of marker genes for each cell cluster (**j**) and  
421 predicted cell type (**k**). The table can be downloaded in CSV format.

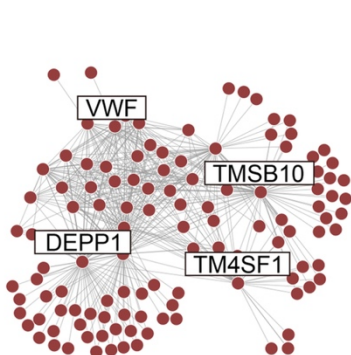
422

423

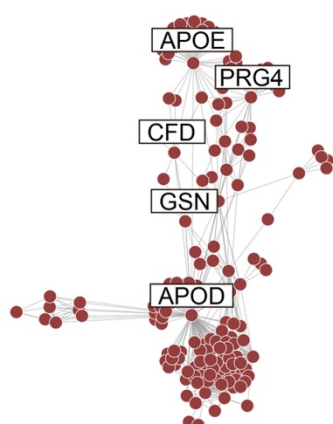
B cell GRN



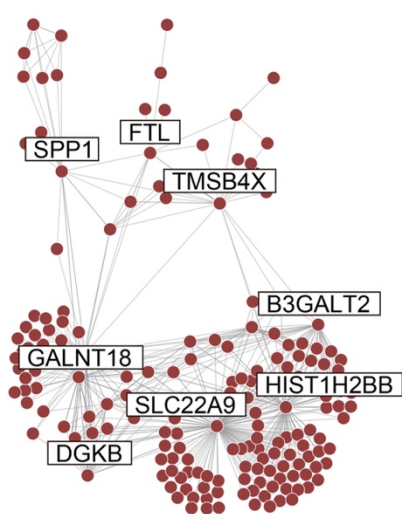
Endothelial cell GRN



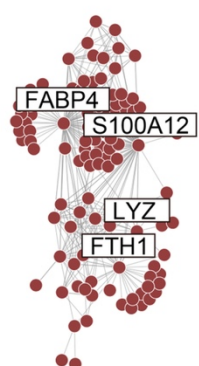
Fibroblast GRN



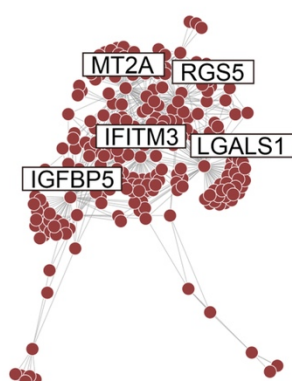
Macrophage GRN



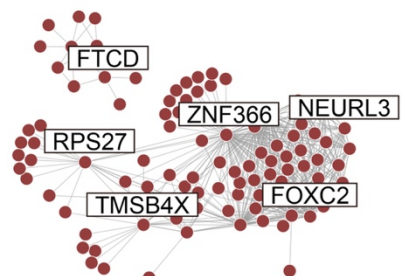
Monocyte GRN



Smooth muscle cell GRN



T/NK cell GRN



424  
425

426 **Supplementary Fig. 8. Gene regulatory networks inferred from scRNA-seq.** Gene networks for each  
427 cell types in Fig. 2a. Red dots represent genes. Core genes are highlighted. Complete and interactive plots  
428 of these GRNs are available online on MSdb database.

429  
430